Design of a Single Orifice Pulse Tube Refrigerator Through the Development of a First-Order Model

by

Alisha R. Schor

Submitted to the Department of Mechanical Engineering in Partial Fulfillment of the Requirements for the Degree of

Bachelor of Science

at the

Massachusetts Institute of Technology

June 2007

Signature of Author.....
Department of Mechanical Engineering
May 11, 2007

Certified by.....
John G. Brisson, II
Associate Professor
Thesis Supervisor

Accepted by.....
John H. Lienhard
Professor, ME Undergraduate Officer

(This page intentionally left blank)

Design of a Single Orifice Pulse Tube Refrigerator
Through the Development of a First-Order Model

by

Alisha R. Schor

Submitted to the Department of Mechanical
Engineering in Partial Fulfillment of the
Requirements for the Degree of Bachelor of Science
in Mechanical Engineering

Abstract

A first order model for the behavior of a linear orifice pulse tube refrigerator (OPTR) was developed as a design tool for construction of actual OPTRs. The model predicts cooling power as well as the pressure/volume relationships for various segments of the refrigerator with minimal computational requirements. The first portion of this document describes the development of this model and its simplifications relative to higher-order numerical models. The second portion of this document details a physical implementation of the pulse tube and compares its performance to the predicted performance of the model. It was found that the model accurately predicted qualitative behavior and trends of the orifice pulse tube refrigerator, but that the predicted temperature difference was approximately five times higher than the measured temperature difference. It is believed that the model can be improved with provisions for flow choking as well as warnings for behavior outside of the accepted operating conditions.

Thesis Supervisor: John G. Brisson, II

Title: Associate Professor, Department of Mechanical Engineering

Acknowledgements

I would like to graciously acknowledge the help of Professor John Brisson, who encouraged me through my work and always took the time to have casual and engaging discussions as well. Professor Joseph Smith was also invaluable in contributing his wisdom and experience to the project, as well as Mr. Michael Demaree, who was generous with his time and knowledge in the machine shop.

Contents

1 Introduction

The pulse tube refrigerator is one of the most prominent types of cryocoolers available today, due to its simplicity and ability to achieve cryogenic temperatures. Several forms of pulse-tube refrigerators exist, but all operate on the Stirling refrigeration cycle and contain the same basic elements: a pressure oscillator, hot and cold heat exchangers, a Stirling-type regenerator, a pulse tube, and a pressure reservoir. Variations between refrigerators can come in the shape and orientation of the pulse tube, the choice of working fluid, the pressure source, and the gas flow path. Pulse tube refrigerators also exist in either single or double orifice varieties, the latter of which allows a small fraction of gas to bypass the regenerator, reducing losses due to pressure drop [1]. Discussion in this document will be limited to the single orifice pulse tube refrigerator (OPTR).

1.1 Single Orifice Pulse Tube Refrigerator (OPTR)

A schematic for the OPTR is shown in Figure 1. The OPTR operates primarily on the Stirling cycle. In fact, an OPTR is simply a Stirling refrigerator with the mechanical expander replaced by the pulse tube.

As with a Stirling refrigerator, gas, typically helium, nitrogen or air, is put through a periodic pressure oscillation using a driver at one end of the refrigerator. At this stage, the gas is at high temperature, T_h (ambient temperature). The gas is then forced through a regenerator, typically stainless steel mesh screens or lead shot, where thermal energy is absorbed such that the exiting gas is at a colder temperature, T_c. This cold gas then travels through the cold heat exchanger, where the gas inside is expanded isothermally, driving a heat flux into the system, denoted $\dot{Q}_c$ in Figure 1.

The expansion is driven by the pulse tube, warm heat exchanger, orifice and pressure reservoir, which

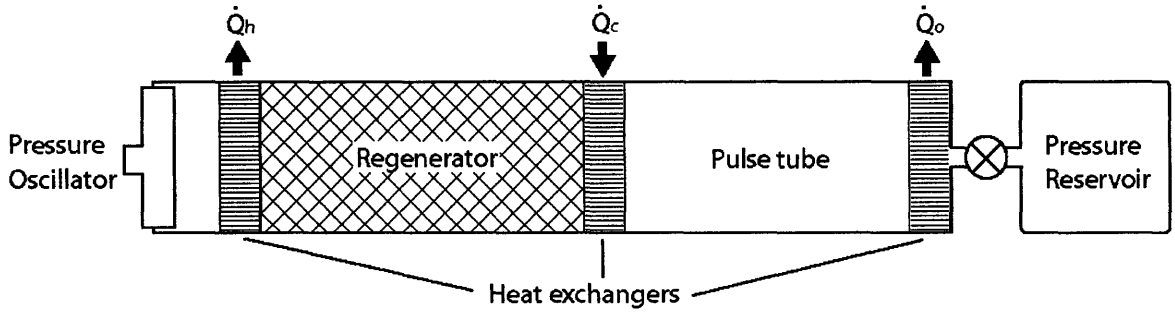

Figure 1: Schematic showing the general layout of an orifice pulse tube refrigerator.

make up the remainder of the system. The orifice provides a resistance to the gas flow; the pressure reservoir is a capacitive element. Together, these create an effective spring-mass-damper system and create a phase shift between mass flow rate and pressure. The heat exchanger between the pulse tube and the throttle is included to dissipate the entropy generated in the throttle.

The pressure reservoir is designed with a volume large enough such that it remains at an average pressure, P_o, throughout the pressure cycles of the refrigerator. The orifice, meanwhile, is sized to decrease the flow between the pulse tube and pressure reservoir, ensuring that not all of the gas in the pulse tube is forced out of the tube. The pulse tube is the primary component of this system. It is designed with sufficient length such that an oscillating slug of gas maintains a separation between the warm and cold ends of the refrigerator. With the aid of flow straighteners, this slug of gas can be viewed as essentially unmixed with the gases at either end, and the result is that the oscillating gas through the orifice/pressure reservoir appears to behave in the same way that a mechanical expander would in a traditional Stirling refrigerator. (It should also be noted that early pulse tube refrigerators relied the heat generated in and dissipated out of the pulse tube only to create a phase shift, without the aid of the orifice and pressure reservoir.) Further detail on the behavior of each component in the OPTR is described in Section 2.

1.2 Existing OPTRs and their applications

Due to their high efficiency at large temperature differences, pulse tube refrigerators are frequently used in cryocooling applications. Early on, the most prominent use of pulse tube refrigerators was by the military, to cool infared cameras [1]. Currently, a number of research institutes (primarily Lockheed Martin, National Institute of Standards and Technology-NIST and Los Alamos National Labs [1]) pursue the development of pulse tube cryocoolers for academic interest, as well as for applications in space. Commercial applications include refrigeration of charcoal adsorbent beds in the semiconductor fabrication industry [1] as well as the liquefaction of helium and nitrogen, for various applications. In many cases, pulse tube refrigerators are being explored as alternatives to current cryocoolers, as they have the advantage of having no moving parts at low temperatures.

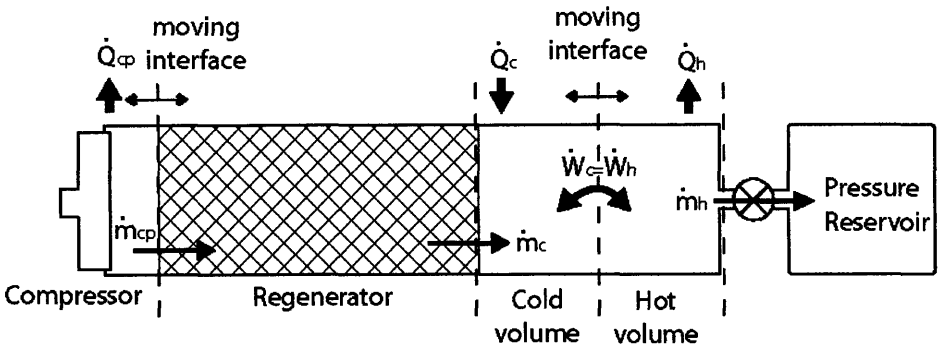

Figure 2: Schematic showing a common division of pulse tube elements and relationships between them. First and second law equations are integrated numerically over each cycle to predict cooling power and required work. The five elements analyzed are the compressor, regenerator, cold volume, hot volume, and pressure reservoir. The cold and hot volumes make up the pulse tube. [2]

2 Model

The major elements of the OPTR, as described in Sec. 1.1, are the pressure oscillator, regenerator, warm and cold heat exchangers, pulse tube, orifice, and pressure reservoir. Numerical models typically analyze these elements by following the entropy flow through five segments: the compressor (or pressure oscillator), the regenerator, a cold volume (including the cold heat exchanger and cold end of the pulse tube), a warm volume (including the warm heat exchanger and warm end of the pulse tube), and the pressure reservoir [2].

Energy and entropy conservation equations can be written for each of these segments separately, with interaction via either work exchange or mass flow across the system boundaries (Figure 2). Note that because pressure oscillates in a cyclic manner, all energy and entropy considerations are taken as averages over a cycle. Entropy generation included in such models come primarily from the regenerator, with the pressure source also contributing a large portion of loss. The throttling at the orifice also leads to some entropy generation, although this has been shown to be significantly less than the regenerator and is typically included in the models [2].

However, models of this form are computationally intensive and often have convergence issues in response to very small changes in parameters. They are difficult to understand on a general level and require extensive knowledge of pulse tube phenomena and behavior in order to "tune"the model to give a meaningful solution.

In this work a simple, first-order model that relates the driving pressure oscillations to volume oscillations at specific points along the refrigerator and uses this relationship to determine the cooling power is developed. Such a model has not currently been published and has the clear advantage of presenting a closed-form

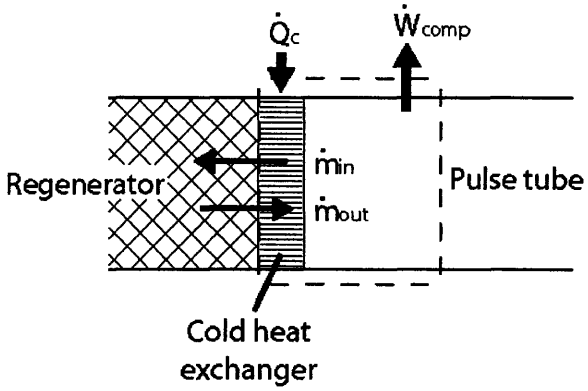

Figure 3: Control volume used to determine the cooling power of the refrigerator. This control volume has a fixed, permeable membrane between the heat exchanger and the regenerator, and moving, impermable membrane that travels in within a small region at the cold end of the pulse tube. The First Law is used to relate $\dot{Q}_c$ and the volume change of the control volume.

solution based on the most basic design parameters. With this model, one can design the major components of a single orifice, pulse-tube refrigerator and iterate through various combinations of sizes in significantly less time (computation time of less than one second compared with several minutes for more complex models), making this a useful tool for preliminary design of systems and even sufficient to produce a working model.

2.1 The First-Order Model

The primary design objective of a refrigerator is, obviously, its cooling power. As described in Section 1.1, the cooling in an OPTR occurs via the expansion at the cold heat exchanger, as in a Stirling refrigerator. However, unlike a Stirling machine, there is no mechanical expander but rather a volume of gas in the pulse tube that acts as a "compressible displacer"[3]. The displacement of this slug of gas within the pulse tube performs a work transfer between the cold and hot ends, and thus conservation of energy is used to determine the cooling power. Figure 3 shows the energy and mass flows through a control volume including the cold heat exchanger and small portion of the pulse tube. The control surface between the regenerator and cold heat exchanger is fixed but permeable, whereas the control surface at the cold end of the pusle tube moves but is impermeable. The amplitude of motion of the moving membrane is small and stays in a volume of fixed temperature, T_c.

The time-varying form of the First Law, written below, is applied to this control volume.

$$\frac{dE}{dt} = \dot{Q} - \dot{W} + \sum_{in} \dot{m}h - \sum_{out} \dot{m}h \tag{1}$$

As shown in Figure 3, $\dot{Q} = \dot{Q}_c$ and $\dot{W}$ is the rate of expansion work performed by the displacer. The relationship between (compression or expansion) work , pressure and volume in oscillating flow is a commonly encountered term and can be expressed as $W = \frac{1}{2} P_a V_a sin(\phi)$, where ϕ is the phase shift between pressure and volume flow, and P_a and V_a represent the amplitudes of oscillation for pressure and volume, respectively. (For reference, this is derived in Appendix C.) The rate at which work is done is simply $\dot{W} = W \times f$, where f is the frequency of oscillation.

Enthalpy flow is considered next. Between the regenerator and the cold heat exchanger, the net enthalpy flow is zero, even though there is mass flow. In an ideal regenerator the temperature exiting near the cold heat exchanger is always T_c. In addition, the cold heat exchanger is assumed to be isothermal, also at T_c. Thus, assuming that there is no dead space between the regenerator and cold heat exchanger, $T_{out} = T_{in} = T_c$ for the mass flow on the regenerator side of the control volume shown in Figure 3. Also, for an ideal gas, $h = c_p T$, and therefore $h_{out} = h_{in}$. Lastly, the cyclic behavior of the system gives that $\dot{m}_{in} = \dot{m}_{out}$, and therefore there is no net enthalpy flow between the cold heat exchanger and the regenerator. On the pulse tube side, since mass flow is zero, there is clearly no enthalpy flow.

Finally, the change in energy over a cycle, $\frac{dE}{dt}$ is zero. Substituting, Eq. 1 can be rewritten as

$$0 = \dot{Q}_c - f\frac{1}{2} P_a \Delta V_a sin(\phi) + 0 \tag{2}$$

which is easily rearranged to give

$$\dot{Q}_c = f\frac{1}{2} P_a \Delta V_a sin(\phi) \tag{3}$$

A similar approach is used to find the work required to drive the OPTR. In fact, the relationship given above, $W = \frac{1}{2} PV sin(\phi)$, gives the work directly, taking the entire OPTR as the control volume, such that

$$\dot{W} = f\frac{1}{2} P_a \Delta V_a sin(\phi) \tag{4}$$

However, it is important to realize that the volume changes, ΔV_a and phase shifts, ϕ, between pressure and volume are *not* the same for Eqs. 3 and 4. The phase shift between pressure and volume at the inlet of the OPTR, used to find the work, is different than the phase shift at the cold heat exchanger, used to find the cooling power, as a result of the compressibility of the working fluid. By the same reasoning, the amplitude of volume oscillations are different at these two points. The following describes how, given a number of simplifying assumptions, conservation equations can be applied to appropriate control volumes

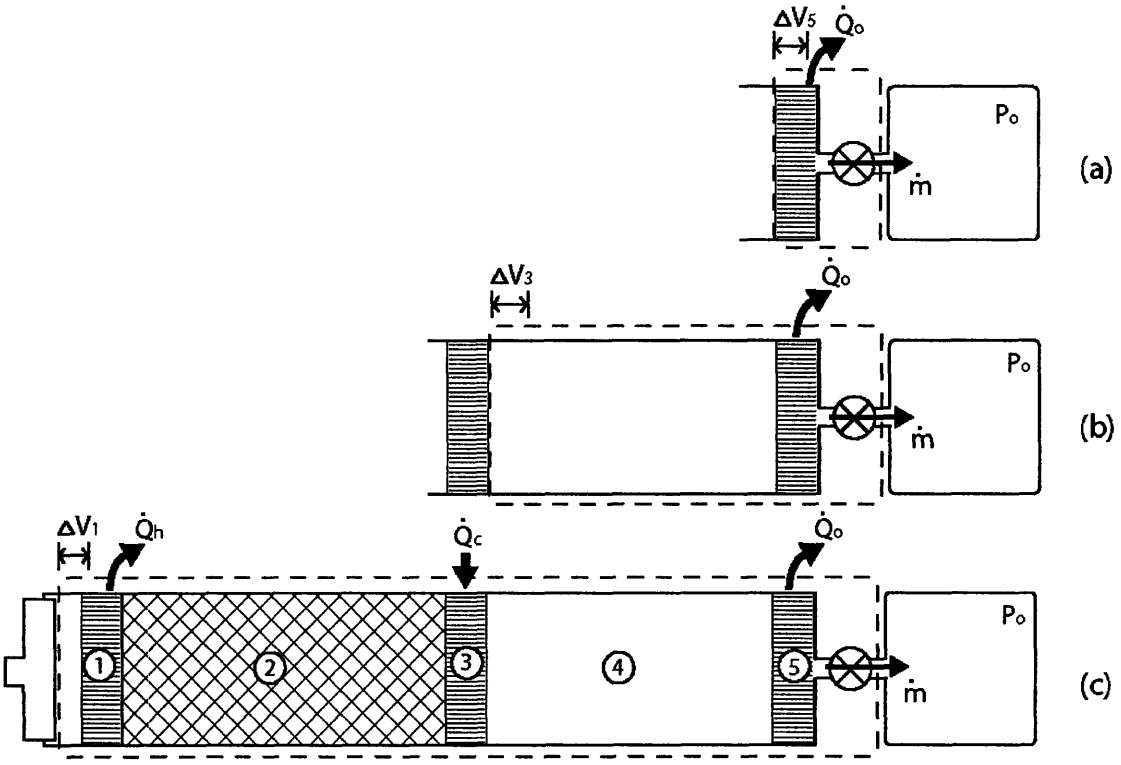

Figure 4: Control volumes used in comparing pressure amplitude in the pulse tube to volume change at various points. (a) Shows the control volume used to find the amplitude of oscillation at the hot heat exchanger. (b) Includes both heat exchangers and the pulse tube, and gives the oscillation of air just behind the regenerator. (c) Includes all the thermodynamic elements of the refrigerator and correlates the input volume oscillation with the input pressure. (c) Also shows the numbering scheme for the refrigerator elements used throughout this analysis.

such that the driving pressure oscillation can be related to an oscillatory volume change at the given control surfaces.

In this approach, the refrigerator is modeled with a series of larger and larger control volumes, as shown in Figure 4. All of the control volumes have a fixed end between the orifice and pressure reservoir, with the opposite control surface being "free"or oscillating, represented by the ΔV symbol. Note that in the figure, the volume oscillations are drawn only in a representative form, and not to scale. Furthermore, for simplicity, the subscript a, signifying amplitude, has been dropped, such that all numbered volume changes (ΔV_1, ΔV_3, ΔV_5) represent an amplitude of oscillation. The amplitudes of both pressure and volume are assumed to be small.

For convenience, the elements of the OPTR have been numbered. As shown in Figure 4, the elements

are: (1) warm heat exchanger, (2) regenerator, (3) cold heat exchanger, (4) pulse tube and (5) dissipative heat exchanger. Figure 4 also shows that all of the oscillating control surfaces are associated with the three heat exchangers (and are labeled correspondingly: $\Delta V_1, \Delta V_3, \Delta V_5$). The reasoning for this is described in the preceding explanation of cooling power.

As described above, the cold heat exchanger is modeled as having varying volume to account for the work transfer from the moving displacement gas. Similarly, the warm end of the pulse tube must also be modeled in the same way, since the heat rejection occurs at the hot end via compression. Also, as with the cold heat exchanger, this heat exchanger is taken to be at a constant temperature (T_h). Thus, the displacement of the gas in the pulse tube is accounted for by ΔV_3 and ΔV_5. The heat exchanger prior to the regenerator is also modeled as isothermal and with oscillating volume, since it is assumed that the compression work from the pressurized input fluid is transferred here.

This model is based on a number of other important assumptions as well. While they do omit a number of fairly significant losses and phenomenon, they are reasonable enough to provide a rough estimate of the primary design parameters—required work and cooling power—based on the sizing of each element shown in Figure 1. These assumptions are as follows:

1. Pressure and volume oscillations are small and sinusoidal: $\Delta P = \Delta P_a e^{i\omega t}, \Delta V = \Delta V_a e^{i\omega t}$.
2. The gas inside the refrigerator is an ideal gas.
3. Mass flow through the orifice, $\dot{m}$, is a function of the pressure amplitude and the average density, ρ_o: $\dot{m} = k\rho_o \Delta P$.
4. The regenerator is ideal, such that the gas entering the warm end is always at T_h and the gas exiting at the cold end is always at T_c. Furthermore, from [4], the regenerator temperature can be viewed as a constant effective regenerator temperature, $T_r = (T_h - T_c)/ln(T_h/T_c)$.
5. The pulse tube itself is adiabatic and isentropic, such that $PV^\gamma = constant$.
6. As mentioned above, heat exchangers are at constant temperature and have variable volume.

Using these assumptions and applying conservation of mass to each control volume, the relationship between the pressure oscillations and volume oscillations at the surface of each heat exchanger is determined.

For each control volume, $\frac{dM_{cv}}{dt} = -\dot{m}_{orifice}$, where M_{cv} is mass of the given control volume. Using the convention in Figure 4, $M_a = M_5, M_b = M_5 + M_4$, and $M_a = M_5 + M_4 + M_3 + M_2 + M_1 = M_{optr}$. Since

the gas inside the OPTR is taken to be ideal and the temperature of element 1, 2, 3, and 5 are taken to be constant (using the effective regenerator temperature T_r), the mass of each of these elements can be expressed as $M_i = PV_i/RT_i$, where i is the element index (as defined in Figure 4), P is the time-varying pressure within the element, V is the time-varying volume, R is the ideal gas constant (mass basis) and T is the temperature of the element. The pulse tube mass, however, must be expressed using the definition $M_4 = V_4(\rho)$, since temperature is not uniform.

Both the pressures and volumes of each element are oscillatory and can be expressed as the sum of an steady and varying value, such that $P_i = P_o + \Delta P_i$ and

$$\begin{aligned}
\Delta V_1 &= V_{1,o} - \Delta V_1 \\
\Delta V_2 &= V_2(fixed) \\
\Delta V_3 &= V_{3,o} + \Delta V_3 \\
\Delta V_4 &= V_{4,o} - \Delta V_3 + \Delta V_5 \\
\Delta V_5 &= V_{5,o} - \Delta V_5
\end{aligned}$$

In the volume relations listed above, the subscript o denotes the original (unpressurized) volume of each element. P_o, on the other hand, is the average pressure during the pressure oscillation, which is typically higher than atmospheric pressure.

In addition, pulse tube density can be written as $\rho = \rho_o + \Delta\rho$. Using the the Ideal Gas Law ($PV = mRT$) and the adiabatic, isentropic assumption ($PV^\gamma = Constant$), $\Delta\rho$ can be rewritten as $P/\rho^\gamma = constant$, and change in density can be shown to be $\Delta\rho = \frac{\rho_o \Delta P}{\gamma P_o}$. The transformation is shown in Appendix A.

The identities for pressure, volume and density given above are then substituted into the conservation of mass equations for each control volume, as appropriate. Since both pressure and volume are time-varying, $\frac{dM}{dt}$ will include non-linear terms for many of the elements. However, since both pressure and volume oscillations are taken to be small, a first-order model is adequate and non-linear terms are dropped. The result is the following set of relationships. The derivation is detailed in Appendix B.

$$\Delta V_{5a} = a\Delta P_a \tag{5}$$

$$\Delta V_{3a} = b\Delta P_a \tag{6}$$

$$\Delta V_a = c\Delta P_a \tag{7}$$

where

$$a = \frac{RT_h}{P_o}\left(\frac{V_{5,o}}{RT_h} + \frac{k\rho_o}{i\omega}\right) \tag{8}$$

$$b = a + \frac{V_{4,o}}{\gamma P_o} + \frac{V_{5,o}}{\rho_o RT_h} - \frac{2}{\rho_o}\left(\frac{V_{5,o}}{RT_h} + \frac{k\rho_o}{i\omega}\right) + \frac{k}{i\omega} \tag{9}$$

$$c = \frac{RT_h}{P_o}\left(\frac{V_{1,o}}{RT_h} + \frac{V_2}{RT_r} + \frac{V_{3,o}}{RT_c} + \frac{bP_o}{RT_c} - b\rho_o + a\rho_o + \frac{V_{5,o}}{RT_h} + \frac{\rho_o V_{4,o}}{\gamma P_o} - \frac{aP_o}{RT_h} + \frac{k\rho_o}{i\omega}\right) \tag{10}$$

These relations give the volume oscillations throughout the OPTR as a function of the inlet pressure oscillation. They also demonstrate that the volume and pressure oscillations are related by a complex number, indicating that there is both a change in magnitude (which should be obvious, since pressure swings are on the order of 10^4 Pa and volume changes are approximately $10^{-6}m^3$) and a phase shift, as desired. Examining the constants a, b and c also shows these phase and magnitude shifts to be dependent on all of the following: refrigerator geometry, working fluid properties, and the mass flow rate tuning constant, k (described in the assumptions above). Of these properties, k is designated as the "tuning constant"since it is the parameter that is both most easily varied (valve choices can be changed even after the rest of the refrigerator has been constructed) and has the highest resolution of change (mass flow rate through a given valve can be varied by opening and closing the valve to various degrees).

The angle of the complex constants a, b and c give the phase shift at each of the three heat exchangers. Eqs. 3 and 4 give cooling power and required work, respectively, as a function of phase shift at a particular point. As mentioned, $\dot{Q}_c$ is calculated by using the phase shift at the cold heat exchanger. Using the constants just derived, this phase shift, $\phi_3 = \angle b$. Similarly, the phase shift that the work is calculated from is $\phi_1 = \angle c$. Thus, Eq. 3 is based on ΔV_3 and ϕ_3, while Eq. 4 is calculated using ΔV_1 and ϕ_1.

The preceding discussion highlights how a first order model is developed to predict the cooling power and required work input for an orifice pulse tube refrigerator based on component sizing, working fluid, input pressure oscillation (frequency and amplitude) and k, a constant used to describe the degree of throttling

between the pulse tube and pressure reservoir. In using this model to design an OPTR, sizing and working fluid can be taken to be limited by "external "constraints—desired overall size and gas availability—such that k, pressure amplitude, and frequency of oscillation are the variables that can be easily manipulated, after the pulse tube has been constructed to give a desired cooling power and temperature difference.

2.2 Limitations of the Model

This model of an orifice pulse tube refrigerator makes a number of gross assumptions that limit its accuracy in predicting cooling power. The largest source of error in this model is the assumption of essentially no losses. In making this assumption, entropy generation in all components (with the exception of the throttle, which is inherently lossy), is taken to be zero. However, friction losses, imperfect thermal recovery within the regenerator and unintentional heat transfer into and out of other metal elements, such as the valve manifold or pressure reservoir, will also contribute losses not included in the model. In addition, the heat exchangers have been assumed to be isothermal and the regenerator is characterized by a known temperature gradient, which are simplifications of the actual thermal behavior.

3 Design of Physical System

A small, solenoid-driven OPTR was designed, constructed and run based on the model presented above. The design considerations for this refrigerator were slightly different than most, since the objective is primarily academic interest. Typically, OPTRs are designed to produce a desired cooling power based on a given or available input power. Small pulse tube refrigerators will provide cooling on the order of 1 watt with inputs of 10 watts, while the largest can draw up to 2kW. However, for this OPTR, the primary goal was to produce a system of reasonable size for demonstration purposes. The sizes chosen were somewhat arbitrary, although diameters were chosen to match existing pipe sizes. Practical limits influenced the size of the pulse tube and pressure reservoir relative to other components; the pulse tube volume must be large enough to prevent thermal mixing, while the pressure reservoir must be large enough to remain at essentially constant pressure. To ensure the former, a pulse-tube volume of at least twice the *gas displacement amplitude*, which is equal to the amplitude of gas velocity divided by angular velocity ($2\pi f$) is desired [5]. Gas velocity amplitude is determined simply by dividing the volume amplitude by the cross sectional area of the tube.

Component sizes based on these parameters are shown in Table 1. The pulse tube and regenerator are constructed from PVC; the regenerator is filled with #6 lead shot (0.110" in diameter) for heat absorption.

Table 1: Summary of dimensions and materials used in the OPTR.

Component	Material	Diameter (in)	Length (in)
Warm Heat Exch.	Copper	3/4 nominal	0.7
Regenerator	PVC, lead	1.25 nom.	6.0
Cold Heat Exch.	Copper	3/4 nom.	0.7
Pulse Tube	PVC	1.25 nom.	7.0
Dissipative Heat Exch.	Copper	3/4 nom.	0.7
Pressure reservoir	Copper	3.5	na

The pressure reservoir must have sufficient volume to withstand the pressure oscillations of the driver, but not so large that the displacement gas leaves the pulse tube. Rotundo et. al. fabricated a similarly sized OPTR for classroom demonstration using a 3.5" copper tank float ($3.7 \times 10^{-4} m^3$) as their pressure reservoir [6]. Since the total volume of the preceding components (heat exchangers, regenerator and pulse tube) is less than $2.13 \times 10^{-4} m^3$, this volume was considered sufficient.

The heat exchangers are copper tubes filled with stacked 50 mesh copper screens. Stacked screen heat exchangers are commonly used in cryocoolers. The goal of these heat exchangers is to maximize radial heat conduction (i.e. between the fridge working fluid and outside environment), while minimizing axial heat conduction, since thermal mixing between components is undesirable. The radial heat transfer of a stacked screen can be predicted by modeling each thread of the screen as two adiabatic-tipped fins (Figure 5). Although there is some conduction between threads, this can be neglected since the area of contact across threads is small (woven threads make contact tangentially).

The heat transfer for an adiabatic-tipped fin is given as [7]:

$$\dot{Q} = M(T_b - T_\infty) tanh(mL) \tag{11}$$

where L is the length of the fin, and M and m are defined as

$$M = \sqrt{hPA_c k} \tag{12}$$

$$m = \sqrt{\frac{hP}{kA_c}} \tag{13}$$

In these definitions, h is the convection coefficient between the fin and the working fluid ($\frac{W}{m^2-K}$), k is the conduction coefficient of the fin ($\frac{W}{m-K}$), and P and A_c are the wetted perimeter and cross-sectional area of

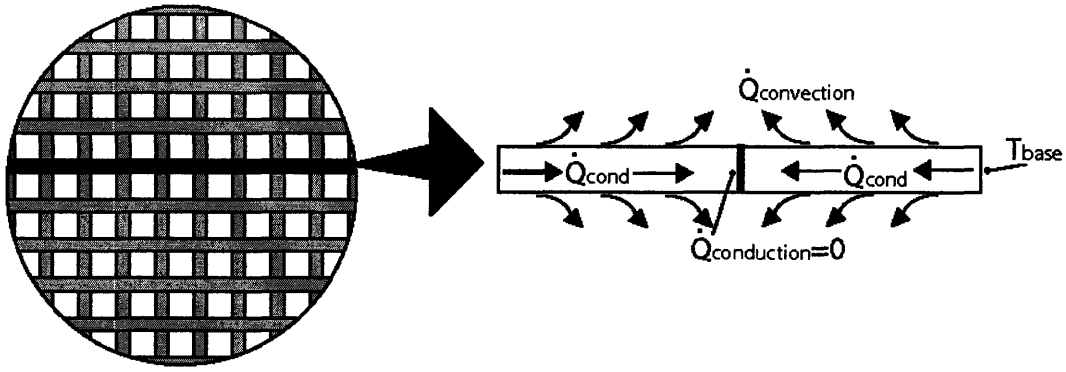

Figure 5: Schematic of a disc of copper screen inside a heat exchanger. (Not to scale.) Each thread of the screen can be modeled as two separate adiabatic-tipped fins, as shown.

the fin, respectively. Since the screens are cut into discs, it is clear that L for each fin is different; however, an average length of $L_{av} = \pi D/2$ can be used.

This heat transfer is then compared to the desired external heat transfer. Assuming that the mode of heat transfer between the outside surface of the heat exchangers are primarily convection, the heat transfer goes according to Newton's Law of convection, $\dot{Q} = hA\Delta T$, where in this case,

$$\Delta T = T_\infty - T_b \tag{14}$$

The heat exchange of the screens is sufficient when the two quantities are equal; i.e., the heat transferred between the working fluid and the heat exchanger is equal to the heat transferred between the heat exchanger and the environment. By setting Eqs. 11 and 14 equal to each other, the heat transfer of heat exchanger, per screen can be expressed in terms of the diameter of the heat exchanger and the size of the screen:

$$\frac{\dot{Q}}{screen} = T_\infty - T_c \left(\frac{1}{hA_{c,hex}} + \frac{1}{Mtanh(mL_{av})} \right)^{-1} \tag{15}$$

This relation was used to size each heat exchanger. For convenience, all of the heat exchangers were made out of the same diameter copper tube. 50 thread per inch copper screen (0.009" diameter wire) was determined to be sufficient for all heat exchangers.

3.1 Fabrication

As mentioned, standard pipe diameters were used to simplify the fabrication process. Each component was cut from pipe of appropriate material to the length specified above. The pulse tube, simply an open tube, was cut out of 3/4" PVC pipe and required no further modification. To join the copper heat exchangers to each end of the pulse tube, the ends were turned to the diameter of the cooper tube, approximately 0.25" deep. The regenerator was cut to length out of 1.25" PVC pipe and filled with #6 (0.110" diameter) lead shot. Appropriately sized end caps were used to connect mating parts as with the pulse tube. Two layers of woven copper screen (50 mesh) were edge epoxied to each end in order to retain the lead shot within the regenerator. Note that in order to maximize entropy transfer, the heat exchangers on either end of the regenerator should be in direct contact with the end of the regenerator. Thus, additional retaining screens were affixed to the end cap and the both caps were filled with lead shot.

Both the hot and cold heat exchangers were fabricated from 3/4" (nominal) copper pipe. In order to improve heat exchange between the flowing gas inside and the ambient environment, 50 mesh copper screens were soldered into the tubes, as noted above. The screens were cut to have a slight interference fit with the inner diameter of the copper tube using a specially fabricated steel punch. Twenty screens were placed in each heat exchanger in order to maximize heat transfer while still having a reasonable pressure drop. Each screen was spaced out using a ring of copper wire to ensure even heat exchange throughout the entire length of the heat exchanger.

The screens were then soldered into the copper tubes. The interference fit of the screens not only ensured adequate heat exchange but also helped the soldering processes. Instead of fixing each screen individually, all of the screens were soldered at once. This was done by pre-coating the interior of a copper tube with lead-tin solder and flux, and then inserting an entire stack of screens and spacers into the tube. The tube was then heated, and additional solder was flowed onto the end screens to ensure a strong bond. A completed heat exchanger is shown in Figure 6.

The pressure reservoir was simply a 3.5" diameter, 1/8" NPT copper tank float, drilled through the threaded connection to allow gas to flow into the hollow sphere. The tank float was chosen based on the suggestion of [6] for its sufficient volume and its ease in connection with the orifice valve, to be discussed below.

Throttling between the pulse tube and the pressure reservoir was achieved with a standard needle valve. The required flow rate through the valve was determined by the model by calculating the volume flow rate out of the hot heat exchanger (ΔV_5), as described in Sec. 2. For needle valves, flow rate is related to the

Figure 6: Heat exchangers used in this OPTR. 50 mesh copper screens were cut and soldered into 3/4" nominal copper pipe. Each heat exchanger contains 20 screens spaced with 20 gauge copper wire.

valve coefficient, C_v, by the following relation given in the Parker Hanafin Corp. valve selection manual:

$$c_v = Q \times 0.0623 \sqrt{\frac{T \times SG}{P_1^2 - P_2^2}} \tag{16}$$

where standard units are used: flow (Q) in SCFM, pressure (P_1 = upstream, P_2 = downstream) in PSIA and temperature in Rankine. SG is the specific gravity of the working fluid.

Using this equation, C_v was found given the required flow rate and an appropriate valve was chosen. The valve used in this pulse tube was a Parker V4 series needle valve with 1/8" NPT connections (P/N: 2M-V4LK-B).

Finally, all elements were connected either by epoxy or threaded connections, where appropriate, in the sequence shown in Figures 2 and 4. The completed OPTR is shown below in Figure 7.

3.2 Testing

A Clippard 3-way solenoid valve (P/N: ET-3M 24 VDC) was used to switch between drawing pressurized gas and venting to the atmosphere, thus providing the required pressure oscillation. The working fluid used was nitrogen gas, based on its availability as shop air. The solenoid valve size was chosen based on the required mass flow rate at the inlet (ΔV_1), trying to prevent choked flow. The valve was switched using a Microdot, Inc. F230B Waveform Generator (generating a square wave), amplified to 24V with an HP 6825A Bipolar Power Supply/Amplifier.

The pulse tube refrigerator was tested at frequencies between 0.1 Hz and 1 Hz and two input pressures,

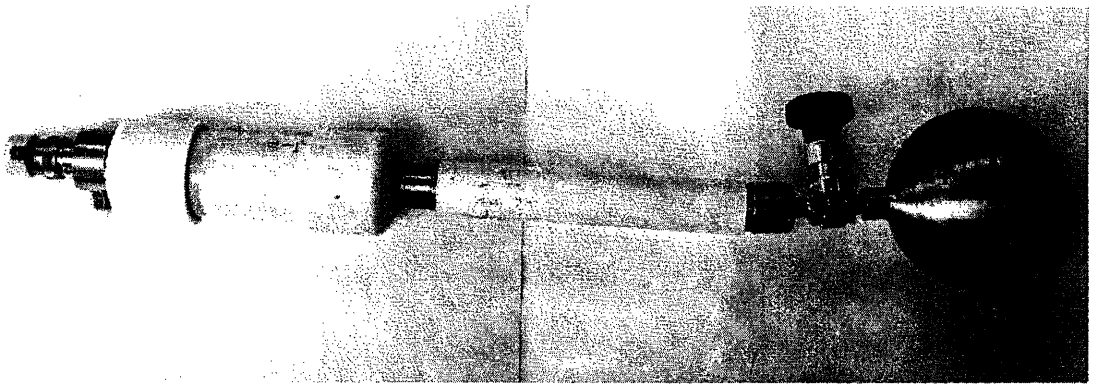

Figure 7: Completed orifice pulse tube refrigerator, without pressure source.

20 psi and 40 psi. Although the original intent was to run the OPTR at frequencies between 1 and 5 Hz (or higher), during the actual implementation, the inlet valve was choked. Thus, the system was run at low frequencies in order to allow sufficient time for the system to pressurize.

For each frequency and pressure combination, the OPTR was run with the throttle valve open to various degrees: 0.5, 2, 4, 6, 8 and 10 turns, with 10 turns being fully open. For each of these data points (combination of frequency, pressure and throttle opening parameters), the system was allowed to run until steady state was reached before the temperature of the cold heat exchanger and the temperature of a reference piece of copper (not connected to the system) were recorded. Ambient temperature was also recorded prior to each test. In addition, testing was repeated with ice on the throttle heat exchanger, in order to observe the effect of improved heat rejection on the cooling power of the OPTR.

4 Results

Behavior of the orifice pulse tube refrigerator was first simulated in MATLAB using the model described above. Two MATLAB files are included in Appendix D. The first, `optrparam.m`, simply defines all the design parameters (size of elements, frequency, pressures) and the material and gas properties. This file also defines a vector for possible values of k, ranging from 10^{-15} to 10^{-2}. This file is run first. `optr.m` is the actual simulation, and first calculates the constants a, b and c (Eqs. 8-10) for each value of k, and then calculates the angle of each constant (i.e. the phase shift at each point.) Using these values and Eqs. 3 and 4, the cooling power and work is then calculated. Note that since k has been previously defined as a vector in `optrparam.m`, all of these parameters are also vectors, which allows the phase shift, input work,

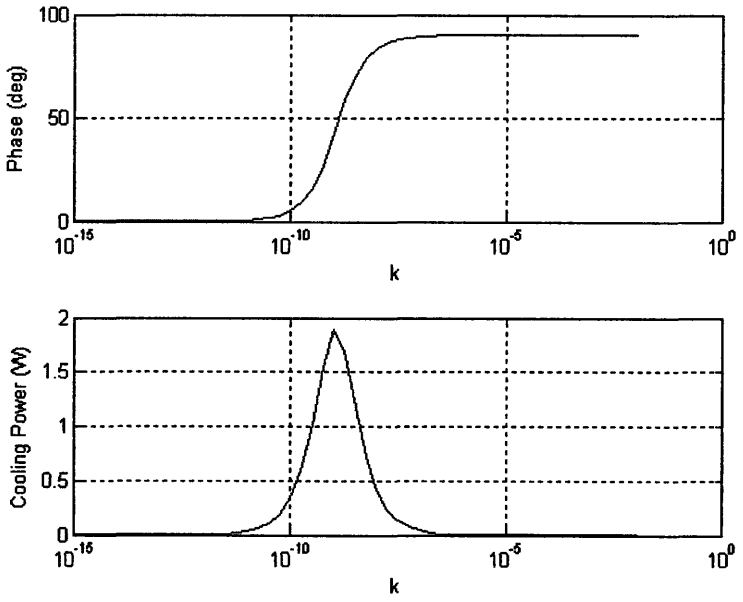

Figure 8: Phase shift and cooling power as a function of k. On the bottom plot, he solid line represents cooling power and the dashed line represents work input. Inputs to this simulation were $f = 1/3$Hz, $P_a = 1.12 \times 10^5$ Pa.

and cooling power to all be plotted as a function of k. A representative plot, shown at a frequency of 1/3 Hz and a pressure amplitude of 1.12×10^5 Pa, is shown in Figure 8.

As shown in the figure, at very low values of k (throttle mostly closed), the phase shift is minimal and cooling power is low. Also, a very high values of k (throttle mostly open), there is a substantial phase lag and cooling power is also low. A peak cooling power occurs at mid-level values of k, where there is some degree of throttling occurring.

The effect of frequency on cooling power and phase shift is shown in Figure 9. Frequencies of 0.1, 0.33, 0.5, 1 and 2 Hz are shown, for the same parameters given above. According to this model, maximum cooling power increases with increasing frequency, as shown, due to the increased mass flow. Also, the phase shifts occur at higher values of k, corresponding with the larger valve opening required to support increased flow.

Results from the physical model are shown below. In each plot, the opening of the throttle valve (measured in number of turns, with 0 being fully closed and 10 being fully open) is plotted against the percentage temperature difference of the cold heat exchanger: $(T_{ref} - T_c)/T_{ref} \times 100$, where T_{ref} is the temperature of a copper block not connected to the OPTR (measured in degrees Fahrenheit). The OPTR was run at various combinations of input pressure and frequency as described in Section 3.2. Under normal conditions,

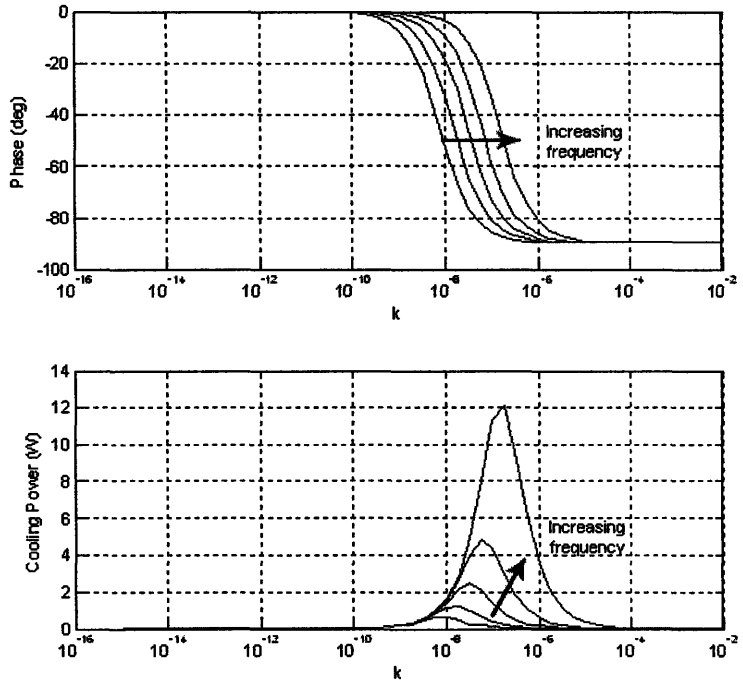

Figure 9: Phase shift and cooling power, as a function of k for frequencies of 0.1, 0.33, 0.5, 1 and 2 Hz.

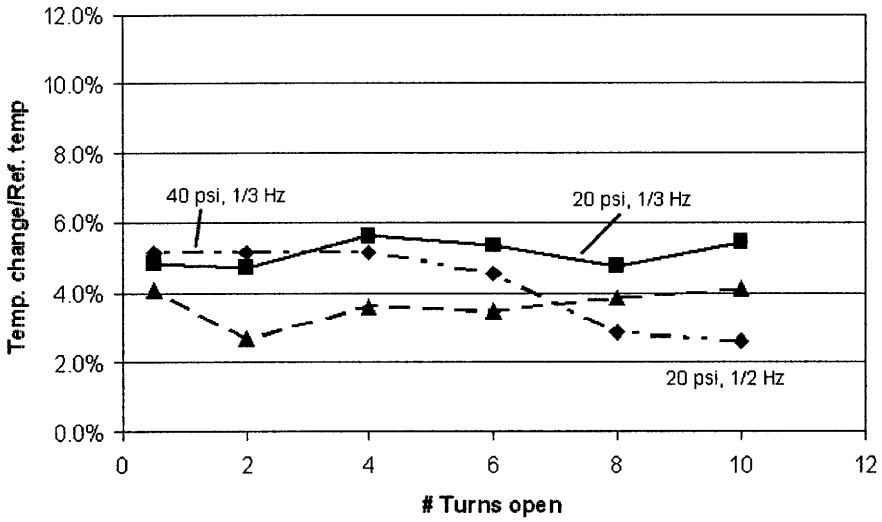

Figure 10: Temperature difference normalized to ambient conditions (degrees Fahrenheit) vs. throttle opening (measured in turns open, 10 being fully open) for three different combinations of input pressure and frequency.

the temperature difference was on the order of 5%, although it did not appear to correlate with the throttling, as expected (Figure 10).

Similar behavior was observed when ice was placed on the heat exchanger between the pulse tube and the throttle, with higher temperature differences (Figure 11).

The lack of effect of the throttle valve opening on cooling generated concerns over whether or not flow into the OPTR (through the Clippard valve) was choked. Pressure measurements at the pressure reservoir confirmed that the average pressure, P_o was lower than expected. Thus, the test was repeated with a valve with a larger opening. The original Clippard valve was replaced with a Clippard EVC-3M-24V-L valve, with a 0.040" orifice, rather than 0.025". This change did significantly improve the behavior of the OPTR, as the bulb pressure was able to reach that of the maximum input pressure. However, it was also noted that at the low frequencies required to minimize choking, the bulb pressure P_o was not actually constant but instead varied between 10 and 15% of the input pressure.

Figures 12 through 14 show the percent temperature difference vs. valve opening with the larger inlet valve. In most of these cases, a peak in cooling power was fairly clear. As before, two inlet pressures were tested at two frequencies each (20 psig maximum pressure, 40 psig, 1/3 Hz and 1/2 Hz). Both the magnitude of and flow coefficient for maximum cooling power were shown to be dependent on both pressure

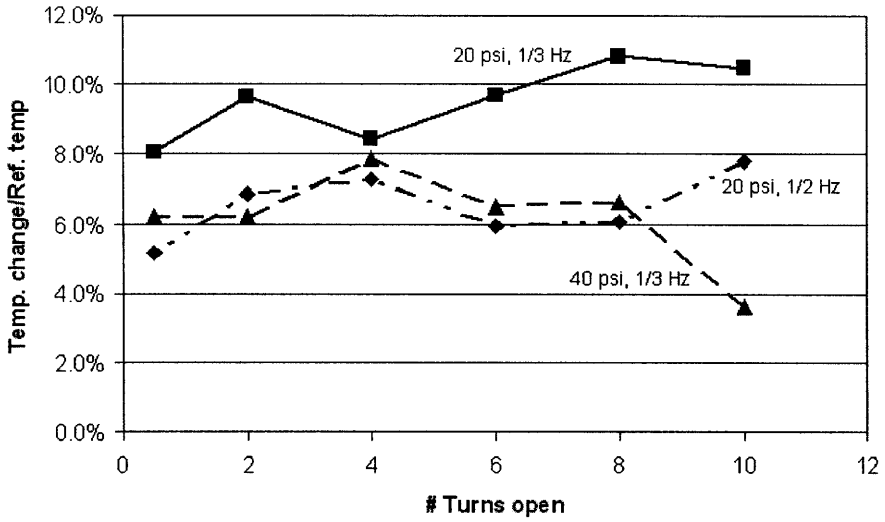

Figure 11: Temperature difference normalized to ambient conditions (degrees Fahrenheit) vs. throttle opening (measured in turns open) with ice on the dissipative heat exchanger. Three different combinations of input pressure and frequency are shown.

and frequency. For the low pressure (20 psig) case, both the maximum and overall cooling powers were lower than those in the high pressure (40 psig) case. However, the effect of frequency on the required valve opening was opposite for the two pressure cases. At low pressures, cooling power peaked with large throttle opening at 1/3 Hz, and required more throttling at 1/2 Hz, whereas in the high pressure case, cooling power peaked with larger throttle opening at 1/2 Hz.

As before, placing ice on the dissipative heat exchanger, prior to the throttle valve, significantly decreased the temperature of the cold heat exchanger relative to the ambient temperature. This effect is shown in Figure 14, which shows the effect of cooling the heat exchanger for inlet conditions of 40psig and 1/3 Hz. Again, cooling power reaches a peak within the operating range of the valve.

5 Discussion

The model predicts a peak in cooling power for mid-level ranges of k (throttle opening), corresponding with a phase shift of 45 degrees. This follows from Eq. 3, which shows that the cooling power depends on phase shift, pressure and volume amplitude. At smaller values of k, the phase shift is small, since a mostly closed throttle will essentially reflect the pressure wave. At these values, cooling power is predicted to be minimal,

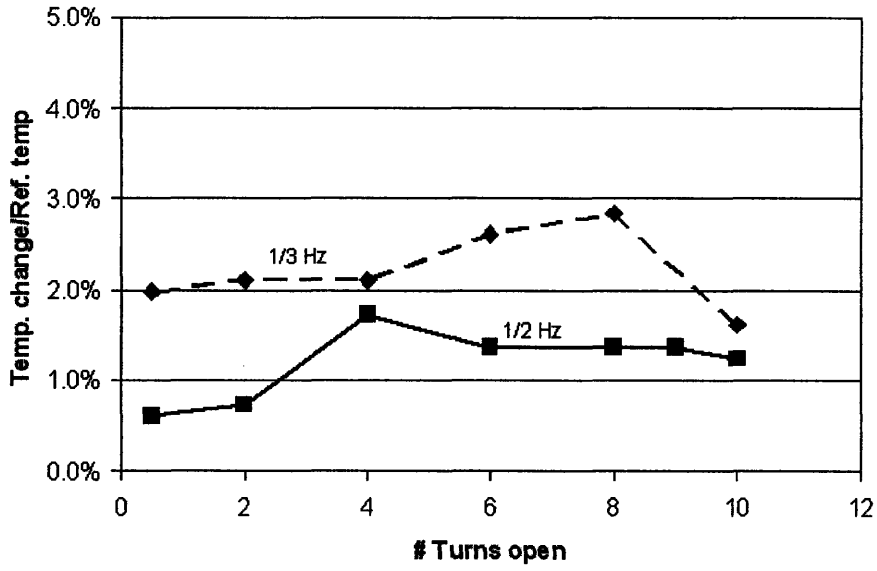

Figure 12: Temperature difference (degrees Fahrenheit) vs. throttle opening (measured in turns open) for an inlet pressure of 20 psig. Frequencies of 1/3 Hz and 1/2 Hz are shown. A slight peak in cooling power can be observed for each case.

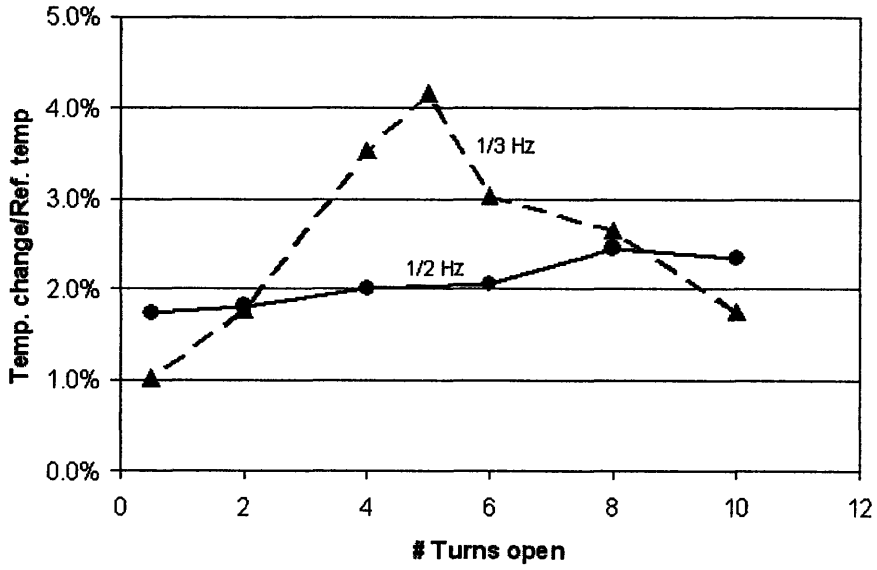

Figure 13: Temperature difference (degrees Fahrenheit) vs. throttle opening (measured in turns open) for an inlet pressure of 40 psig. The peak in cooling power is significantly more pronounced in the case of $f = 1/3$ Hz. The peak cooling power for the 1/2 Hz case is likely at a point of higher flow than the existing valve could handle.

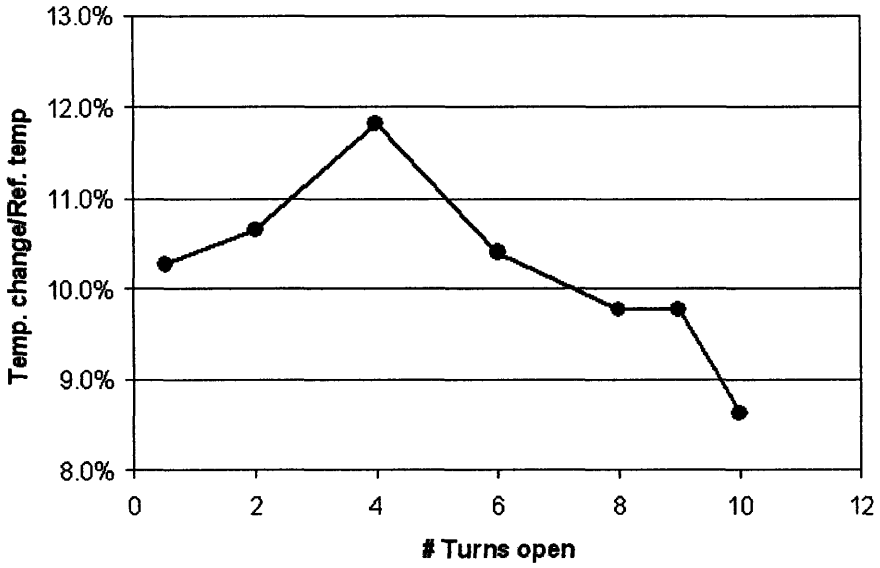

Figure 14: Temperature difference (degrees Fahrenheit) vs. throttle opening (measured in turns open) for an inlet pressure of 40 psig and frequency of 1/3 Hz, with ice on the dissipative heat exchanger. Heat exchange was significantly improved and a peak in cooling power was evident.

both due to the phase shift and also the fact that the amplitude of volume oscillation is smaller with a closed throttle (less total volume being compressed). At large values of k, however, the phase shift approaches 90 degrees, and thus cooling power is expected to be high. However, due to the large opening, pressure amplitudes are small and cooling power stays low at this end of the spectrum.

Data taken from the physical system show similar behavior. Figures 12 through 14 show that in almost all cases, cooling power peaked at some midrange of number of turns open. For the valve used, the turns open vs. c_v plot is shown in Figure 15. The valve coefficient is related to the flow rate by Eq. 16, which can in turn be related to k, since $\dot{m} = k\rho\Delta P$. While the exact value for the valve coefficient is difficult to obtain from the number of turns open, it is clear that the effect of turns open should be similar to that of the constant k, which is observed.

In the 40 psi, 1/2 Hz operating case, however (Figure 13), this behavior was not observed. Although a slight increase in cooling power is noted at eight turns open, cooling power appears to increase consistently with wider valve openings. The most likely cause of this is that at this combination of high pressure and higher frequency, the time constant for pressure equilibration in the reservoir ($\tau \approx RC$) is too slow for the given valve size. In other words, to achieve a response time sufficiently fast for these conditions, R must be

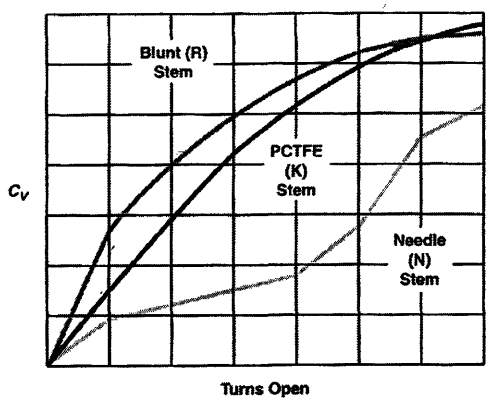

Figure 15: Valve coefficient, c_v related to the number of turns open. The valve used in this system had a PCTFE stem with a maximum c_v of 0.28. (Plot taken from Parker valve catalog)

Table 2: Summary of maximum cooling powers and temperature differences for test cases

Pressure (psi)	Frequency (Hz)	Max. ΔT [°C]	Max $\dot{Q}_c$ [W]
20	1/3	1.3	0.0147
	1/2	0.8	0.00895
40	1/3	1.8	0.0211
	1/2	1.1	0.01215
(iced)	1/3	5.1	0.5882

reduced significantly. However, the resistance of the valve chosen is too high even at full opening, and thus cooling power does not peak in this case. Regardless, the trends of the other plots are clear enough to show a reasonable match with the predicted behavior trends.

Perhaps of greater interest from a design perspective, however, is the model's ability to quantitatively predict the cooling power of the OPTR. Predictions for maximum cooling power were on the order of 1-2 watts, depending on configuration, with a temperature difference of 15° C between the cold heat exchanger and the environment. The actual system produced a best-case cooling power of only 0.06 W, with a temperature difference of 5° C, at 40 psi and 1/3 Hz, with ice on the dissipative heat exchanger (Table 2).

The measured cooling values and temperature differences extremely low compared with the prediction, indicating that there were not only unaccounted losses but that the OPTR was not functioning properly. The most significant result, in trying to investigate this issue, is the fact that there were large pressure oscillations in the reservoir. This suggests that too much gas inside the pulse tube was passing into the pressure reservoir. In a working OPTR, a slug of gas contained within the pulse tube acts as a displacer, oscillating back and forth within the pulse tube in order to transmit work between the cold heat exchanger

and the heat exchanger at the throttle. Also, containing this displacement gas entirely within the pulse tube ensures insulation between the two heat exchangers. If the volume oscillations are too large, the gas slug will pass completely through the pulse tube and the OPTR will lose its cooling ability as warm gas from the throttle will be actively mixed with the gas in the cold heat exchanger.

A rough conservation of mass calculation verifies this phenomenon. Assuming the pressure reservoir to be roughly constant temperature, that fact that P_o is not constant indicates that the mass inside the reservoir is changing ($PV = mRT$). In addition, any additional mass entering the reservoir must come from the pulse tube, i.e. $|\Delta m_{pt}| = |\Delta m_{res}|$. Using the ideal gas law to express mass in terms of other properties and assuming (conservatively) that the reservoir temperature and pulse temperature are both constant and equal, we have that

$$P_{av}(\Delta V_{pt} + V_{res}) = (\Delta P + P_{av})V_{res}, \tag{17}$$

where P_{av} is the average pressure in the pulse tube and OPTR, ΔV_{pt} is instantaneous volume of the displacing gas within the pulse tube, and V_{res} is the fixed reservoir volume. The volume of gas within the pulse tube is related to the length of the displacing gas easily by geometry, $V_{pt} = L(\pi D_{pt}^2/4)$. Substituting and rearranging, the length of travel, L of the displacing gas is expressed as

$$L = \frac{\Delta P}{P_{av} V_{res}} \frac{4}{\pi D_{pt}^2} \tag{18}$$

This length must be significantly shorter than the length of the pulse tube. Using various measured reservoir pressure changes, L was found to vary between 8.0 cm and 15.2 cm. The pulse tube, however, is 7"(17.8 cm) long, and therefore a significant amount of the displacing gas that is escaping through the throttle valve. The measurable but not extreme change in cold temperature when ice was placed near the throttle is consistent this theory. Given these travel lengths, it is likely that the ice cooled a section of gas that was carried down the length of the pulse tube far enough that it mixed with the gas in the cold heat exchanger.

Increasing the length of the pulse tube or decreasing reservoir size would also shorten the travel length of the gas slug. Practically speaking, however, the pulse tube would have to be extraordinarily long to offset the large pressure deviations in the reservoir and decreasing the volume of the reservoir would itself make the reservoir more prone to pressure changes. From Eq. 18, and choosing a reasonable L to be approximately 1 cm, the maximum tolerable pressure change in the reservoir is about 0.1% of the input pressure. This could

be achieved with increased throttling or faster driving frequencies, although as mentioned before, increased input frequency presented additional problems.

6 Conclusion

A first-order model for the behavior of an orifice pulse tube refrigerator was developed and validated through the construction of a physical refrigerator. At low driving frequencies the refrigerator was able to produce some cooling, although the amount was substantially lower than predicted. The low cooling power was likely a result of large volume oscillations within the pulse tube, causing thermal mixing between the warm and cold ends of the pulse tube.

These large volume oscillations were caused by large pressure swings within the pressure reservoir (10-15% of the inlet pressure), which were, in turn, a result of the low running frequencies required to prevent flow choking at inlet of the OPTR. Greater throttling between the pulse tube and pressure reservoir would also reduce these pressure swings. Thus, two major proposals for achieving the desired cooling power are (1) increase the size of the inlet valve and run at higher frequencies and (2) increase throttling. A suggested minimum input frequency is 2 Hz; although in this model, no cooling power was observed at this frequency, testing did show the pressure reservoir to be roughly constant for these conditions.

The model presented above, then, is adequate for describing general behavior and trends in OPTR operation, but overly simplified for actual design of pulse tube refrigerators. In particular, flow limitations and warnings for pulse tube displacement distance are not included. These two factors proved to be the most detrimental to the behavior of the OPTR. While these issues are likely correctly with modifications to the physical OPTR, from the perspective of using the model as a design tool, it would be useful to modify the code to flag these problems. Nevertheless, the current model is useful for preliminary sizing and first-order calculations, with the understanding that there exist some known potential problems and that troubleshooting and modifications would be required to physically implement such a system.

A Isentropic relations for density

The following describes the derivation of the isentropic relationship between $\Delta\rho$ and the input parameters $\Delta P, \rho_o$ and P_o within the pulse tube.

Adiabatic, isentropic relation for an ideal gas:

$$PV^\gamma = constant = P_o V_o^\gamma \tag{19}$$

Since the mass of gas inside the pulse tube is constant, this can be rewritten as

$$\frac{P_o}{\rho_o^\gamma} = constant \times m^\gamma = constant' \tag{20}$$

Expressing the changes in pressure and density as $P_o + \Delta P$ and $\rho_o + \Delta\rho$, respectively, we can write:

$$\frac{(P_o + \Delta P)}{(\rho_o + \Delta\rho)^\gamma} = \frac{P_o}{\rho_o^\gamma} \tag{21}$$

or,

$$(P_o + \Delta P) = \frac{P_o}{\rho_o^\gamma}(\rho_o + \Delta\rho)^\gamma \tag{22}$$

Factoring, we have

$$\left(1 + \frac{\Delta P}{P_o}\right) P_o = \frac{P_o}{\rho_o^\gamma}\rho_o^\gamma \left(1 + \frac{\Delta\rho}{\rho_o}\right)^\gamma \tag{23}$$

P_o and ρ_o^γ can be canceled from both sides of the equation. Approximating using the first order terms from the binomial expansion, this leaves

$$1 + \frac{\Delta P}{P_o} \approx 1 + \gamma\frac{\Delta\rho}{\rho_o} \tag{24}$$

Finally, subtracting 1 from both sides and rearranging, we are left with

$$\Delta\rho = \frac{\rho_o \Delta P}{\gamma P_o} \tag{25}$$

B Phase shift relationships

Using conservation of mass principles, along with the assumptions discussed in Section 2, relationships between pressure amplitude and volume amplitude at three points of oscillation were developed. These expressions are listed as Eqs. 5-10. The constants listed are imaginary numbers describing the phase and amplitude shift between input pressure swings and volume. Derivation of these constants is described in this Appendix. For reference, Figure 4 has been reproduced here.

Beginning with control volume (a), and recalling that $\dot{m} = k\rho_o \Delta P$ and $M_5 = \frac{P_5 V_5}{RT_h}$ we first write a conservation of mass equation for this control volume and make appropriate substitutions.

$$\begin{aligned} \frac{dM_5}{dt} &= -\dot{m}_{out} \\ \frac{d}{dt}\frac{P_5 V_5}{RT_h} &= -k\rho_o \Delta P \end{aligned}$$

Pressure and volume are both time-varying and can be expressed as $P_5 = P_o + \Delta P$ and $V_5 = V_{5,o} - \Delta V_5$. Making these substitutions, taking the time derivative and eliminating non-linear terms,

$$\begin{aligned} \frac{dM_5}{dt} &= \frac{1}{RT_h}\frac{d}{dt}\left((P_o + \Delta P)(V_{5,o} - \Delta V_5)\right) \\ &= \frac{1}{RT_h}\left(\frac{d\Delta P}{dt}(V_{5,o} - \Delta V_5) - \frac{d\Delta V_5}{dt}(P_o - \Delta P)\right) \\ &= \frac{d\Delta P}{dt}\frac{V_{5,o}}{RT_h} - \frac{d\Delta V_5}{dt}\frac{P_o}{RT_h} \\ \frac{d\Delta P}{dt}\frac{V_{5,o}}{RT_h} - \frac{d\Delta V_5}{dt}\frac{P_o}{RT_h} &= -k\rho_o \Delta P \end{aligned}$$

Here, let $\Delta P = \Delta P_a e^{i\omega t}$ and $\Delta V_5 = \Delta V_{5a} e^{i\omega t}$. Substituting this into the equation above and taking the time derivative, we are left with an $e^{i\omega t}$ coefficient in all expressions, which is canceled to give

$$\begin{aligned} i\omega \Delta P_a e^{i\omega t}\frac{V_{5,o}}{RT_h} - i\omega \Delta V_{5a} e^{i\omega t}\frac{P_o}{RT_h} &= -k\rho_o \Delta P_a e^{i\omega t} \\ i\omega \Delta P_a \frac{V_{5,o}}{RT_h} - i\omega \Delta V_{5a}\frac{P_o}{RT_h} &= -k\rho_o \Delta P_a \end{aligned}$$

After some algebra, isolating the ΔP_a and ΔV_{5a} terms, we have

$$\Delta V_{5a} = \left(\frac{V_{5,o}}{P_o} + \frac{k\rho_o RT_h}{i\omega P_o}\right)\Delta P_a$$

as presented in Eqs. 5 and 8 above.

The same procedure is applied to the remaining to control volumes to obtain relationships of a similar form. For control volume (b), $M_{cv} = M_4 + M_5$, where $M_4 = \rho V_4$ and $V_4 = V_4, o - \Delta V_3 + \Delta V_5$. As before,

$M_5 = \frac{P_5 V_5}{RT_h}$. Also, as with pressure and volume above, we assume that the oscillations of density can be expressed as $\rho_o + \Delta\rho$. This gives the total mass in the system as

$$M = (V_4, o - \Delta V_3 + \Delta V_5)(\rho_o + \Delta\rho) + \frac{(P_o + \Delta P)(V_{5,o} - \Delta V_5)}{RT_h}$$

Additionally, $\Delta\rho$ can be substituted with $\frac{\rho_o \Delta P}{\gamma P_o}$ as shown in Appendix A above. Taking the time derivative of the expression above, and eliminating higher order terms,

$$\frac{dM}{dt} = -\frac{d\Delta V_3}{dt}\rho_o + \frac{d\Delta V_5}{dt}\rho_o + \frac{d\Delta P}{dt}\frac{\rho_o V_{4,o}}{\gamma P_o} + \frac{d\Delta P}{dt}\frac{V_{5,o}}{RT_h} - \frac{d\Delta V_5}{dt}\frac{P_o}{RT_h} = -k\rho_o \Delta P$$

Here, the coefficient relating ΔV_{5a} and ΔP_a Eq. 8 can be substituted for $\frac{dV_5}{dt}$. Letting $\Delta P = \Delta P_a e^{i\omega t}$ and $\Delta V_5 = \Delta V_{5a} e^{i\omega t}$, as before, it is straightforward although tedious, algebra to show that

$$\Delta V_3 a = a + \frac{V_{4,o}}{\gamma P_o} + \frac{V_{5,o}}{\rho_o RT_h} - \frac{2}{\rho_o}\left(\frac{V_{5,o}}{RT_h} + \frac{k\rho_o}{i\omega}\right) + \frac{k}{i\omega}$$

The final coefficient, relating pressure and volume at the surface of control volume (c) does not require any further assumptions or creative substitutions. M_{cv} is the sum of the masses of elements 1-5,

$$M_{cv} = \frac{PV_1}{RT_h} + \frac{PV_2}{RT_r} + \frac{PV_3}{RT_c} + V_4\rho + \frac{PV_5}{RT_h}$$

and

$$\begin{aligned}
\Delta V_1 &= V_{1,o} - \Delta V_1 \\
\Delta V_2 &= V_{2,o}(fixed) \\
\Delta V_3 &= V_{3,o} + \Delta V_3 \\
\Delta V_4 &= V_{4,o} - \Delta V_3 + \Delta V_5 \\
\Delta V_5 &= V_{5,o} - \Delta V_5
\end{aligned}$$

As before, we make appropriate substitutions, linearize the time-derivative of mass, and substitute for the oscillating pressure and volume terms. Following these steps and rearranging the subsequent expression to relative ΔV_{1a} to ΔP_a, we have

$$\Delta V_{1a} = \Delta P_a \left\{ \frac{RT_h}{P_o}\left(\frac{V_{1,o}}{RT_h} + \frac{V_2}{RT_r} + \frac{V_{3,o}}{RT_c} + \frac{bP_o}{RT_c} - b\rho_o + a\rho_o + \frac{V_{5,o}}{RT_h} + \frac{\rho_o V_{4,o}}{\gamma P_o} - \frac{aP_o}{RT_h} + \frac{k\rho_o}{i\omega}\right)\right\}$$

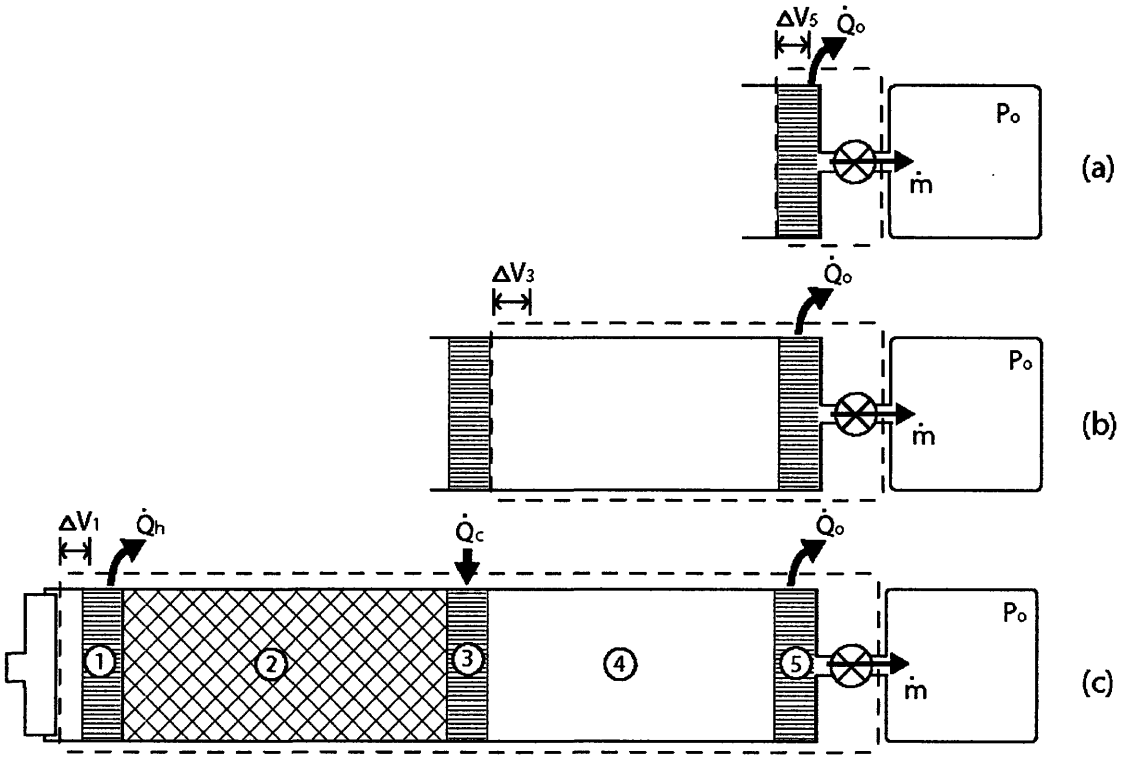

Figure 16: Reproduction of Figure 4. The numbered elements are: (1) warm heat exchanger, (2) regenerator, (3) cold heat exchanger, (4) pulse tube and (5) dissipative heat exchanger.

C Gas compression work

The following details the derivation of the relationship for work: $W = PVsin(\phi)$ from the definition $W = \int PdV$:

Assuming volume and pressure act sinusoidally with a phase lag, ϕ, we can express them as $V = V_a cos(\omega t)$ and $P = P_a cos(\omega t + \phi)$, where V_a and P_a are the amplitudes of volume and pressure oscillation, respectively at the inlet. Taking the first derivative of the volume expression given, we can write $dV = -\omega V_a sin(\omega t)dt$. Substituting these expressions, the expression for work can be rewritten:

$$W = \int P_a cos(\omega t + \phi)(-\omega V_a sin(\omega t))dt \tag{26}$$

$$= -P_a V_a \omega \int cos(\omega t + \phi)sin(\omega t)dt \tag{27}$$

Using the trigonometric identity for cosine addition,

$$W = -P_a V_a \omega \int (cos(\omega t)cos(\phi) - sin(\omega t)sin(\phi))sin\omega t dt \tag{28}$$

$$= -P_a V_a \omega \left\{ \int (cos\omega t sin\omega t)dt cos\phi - \int sin^2(\omega t)dt sin\phi \right\} \tag{29}$$

Substituting in two more trigonometric identities:

$$cos(\omega t)sin(\omega t) = \tfrac{1}{2}sin(2\omega t)$$

$$sin^2(\omega t) = \tfrac{1-cos2\omega t}{2}$$

and integrating around a cycle, we have

$$= -P_a V_a \omega \left\{ cos\phi \left(-\frac{1}{2\omega} cos^2(\omega t) \right) |_0^{\frac{2\pi}{\omega}} - sin\phi \left(\frac{t}{2} - \frac{sin(2\omega t)}{4\omega} \right) |_0^{\frac{2\pi}{\omega}} \right\} \tag{30}$$

$$= -P_a V_a \omega \left\{ -sin\phi - sin\phi \left(\frac{2\pi}{2\omega} - \frac{sin(4\omega)}{4\omega} \right) - \left(\frac{0}{2} - \frac{sin(0)}{4\omega} \right) \right\} \tag{31}$$

The $\sin(4\pi)/(4\omega)$, $\frac{0}{2}$ and $\frac{sin(0)}{4\omega}$ terms are all equal to zero, and $\frac{2\pi}{2\omega}$ simply reduces to $\frac{\pi}{\omega}$, which cancels with the ω in the constant term. Thus, we are left with:

$$W = PV\pi sin(\phi)[rad] = \frac{1}{2}PVsin(\phi)[degrees] \tag{32}$$

D MATLAB Code

```
%Pulse Tube Refrigerator Analysis

%Alisha Schor, alisha.schor@gmail.com

%Define geometric parameters

%All units SI (kg-m-s)


%Inches to meters multiplier

TOSI=0.0254;


%Swept Volume

dswept=1.364*TOSI;

lswept=0.1;

f=2; %Hz

Aswept=pi*dswept^2/4;

w=2*pi*f;

%Aftercooler (first HEX)

do=0.811*TOSI;

lo=0.7*TOSI;

Ao=pi*do^2/4;

Vo=Ao*lo;

%Regenerator

dr=1.364*TOSI;

lr=6*TOSI;

Ar=pi*dr^2/4;

Vr=Ar*lr;

%Cold HEX

dc=0.811*TOSI;

lc=0.7*TOSI;

Ac=pi*dc^2/4;

Vc=Ac*lc;

%Pulse Tube
```

```
dpt=0.81*TOSI;

lpt=6*TOSI;

Apt=pi*dpt^2/4;

Vpt=Apt*lpt;

%Warm HEX

dh=0.811*TOSI;

lh=0.7*TOSI;

Ah=pi*dh^2/4;

Vh=Ah*lh;


%Choose temperatures

Tc=285; %K

Th=300; %K

Tr=(Th-Tc)/log(Th/Tc);


%NOTE: Either properties of air or properties

%of nitrogen must be commented prior to running

%this file.


%Properties of air

% R=287; %J/kg-K

% rhoo=1.229; %kg/m^3

% gamma=1.4;

% Patm=1.01e5; %Pa

% mu=1.5e-5; %Pa-s

% cp=1003; %J/kg-K

% kair=0.02544; %W/m-K

% nu=1.475e-5; %m^2/s


%Properties of nitrogen

R=290; %J/kg-K
```

```
rhoo=1.116; %kg/m^3

gamma=1.4;

Patm=1.01e5; %Pa

mu=1.8042e-5; %Pa-s

cp=1041.4; %J/kg-K

kair=0.02607; %W/m-K

nu=1.6231-5; %m^2/s


%Properties of copper

ccu=385; %J/kg-K

kcu=385; %W/m-K

rhocu=8960; %kg/m^3


%Chosen properties

Po=Patm;

Va=Aswept*lswept;

k=2:0.25:15;

k=10.^(-k);
```

```
   %Pulse Tube Refrigerator Analysis
%Alisha Schor, alisha.schor@gmail.com
%Run optrparam.m first to define parameters

%Time vector
t=0:0.005:2;

for j=1:length(k)
a(j)=R*Th/Po*(Vh/(R*Th)+(k(j)*rhoo/(i*w)));
b(j)=a(j)+Vpt/(gamma*Po)+Vh/(rhoo*R*Th)-1/rhoo*(Vh/(R*Th)+...
(k(j)*rhoo/(i*w))+k(j)/(i*w));
c(j)=R*Th/Po*(Vo/(R*Th)+Vr/(R*Tr)+Vc/(R*Tc)+b(j)*Po/(R*Tc)-...
b(j)*rhoo+a(j)*rhoo+rhoo*Vpt/(gamma*Po)+Vh/(R*Th)-a(j)*...
Po/(R*Th)+k(j)*rhoo/(i*w));
end
phase=angle(c)*180/pi;
MagC=abs(c);

% Calculate work and cooling power by choosing either
% pressure or volume amplitude.
% Pa=Va./MagC or Va=Pa.*MagC
Pa=Va./MagC;
Work=.5.*Pa.*Va.*sin(angle(c))*f;
DV3=Pa.*abs(b);
Qc=abs(-.5.*Pa.*DV3.*sin(angle(b))*f+i*w/(R*Tc)*(Pa*Vc+DV3*Po));

MaxWork=max(-Work)
MaxCooling=max(Qc)

for g=1:length(Work)
if Qc(g)==MaxCooling
```

```
OptimumK=k(g)

OptimumPhase=angle(c(g))*180/pi

MassFlow=OptimumK*rhoo*Pa(g);

VolFlow=OptimumK*Pa(g)

break

end

end


%Plot outputs

figure(1)

subplot(2,1,1)

semilogx(k,phase);xlabel('k');ylabel('Phase (deg)');

grid on

hold on

subplot(2,1,2)

semilogx(k,-Work,'k-.');

hold on

semilogx(k,Qc,'b');

xlabel('k');

ylabel('Cooling Power (W)');

grid on


%Valve sizing and Cv

%Based on Swagelok & Parker references

Q=OptimumK*Pa(g)*2118.88; %CFM

P1=(Po+Pa(g)/2)*0.0001450377; %PSIA

P2=Po*0.0001450377; %PSIA

%SG=1; %air

SG=0.967; %nitrogen T=(Th-273.15)*9/5+32+460; %"Absolute Temperature"

Cv=Q/16.05*sqrt(SG*T/(P1^2-P2^2))
```

```
%Required nozzle size based on mass flow rate

Pup=60; %upstream pressure in psi

Pup=Pup*6894.757; %upstream pressure in Pa

Anoz=MassFlow/(gamma^.5)*(2/(gamma+1))^(-(gamma+1)/(2*gamma-1))*sqrt(R*Th)/(Pup);

Dnoz=sqrt(4/pi*Anoz)
```

References

[1] R. Radebaugh, "Development of the pulse tube refrigerator as an efficient and reliable cryocooler," 1999-2000.

[2] P. Neveu and C. Babo, "A simplified model for pulse tube refrigeration," *Cryogenics*, vol. 40, no. 3, pp. 191–201, 2000/3.

[3] P. Kittel, A. Kashani, J. M. Lee, and P. R. Roach, "General pulse tube theory," *Cryogenics*, vol. 36, no. 10, pp. 849–857, 1996/10.

[4] I. Urieli and D. M. Berchowitz, *Stirling Cycle Engine Anaylsis.* Bristol: Adam Hilger Ltd., 1984.

[5] G. Swift, *Thermoacoustics: A unifying perspective for some engines and refrigerators.* Los Alamos National Laboratory: Unbublished, 2001.

[6] S. Rotundo, G. Hughel, A. Rebarchak, Y. Lin, and B. Farouk, "Design, construction and operation of a traveling-wave pulse tube refrigerator," in *14th International Cryocooler Conference*, June 2006.

[7] F. P. Incorpera and D. P. DeWitt, *Heat Transfer From Extended Surfaces*, ch. 3.6, p. 126. Fundamentals of Heat and Mass Transfer, Hoboken, NJ: John Wiley and Sons, 5th ed., 2002.

[8] S. Choi, K. Nam, and S. Jeong, "Investigation on the pressure drop characteristics of cryocooler regenerators under oscillating flow and pulsating pressure conditions," *Cryogenics*, vol. 44, no. 3, pp. 203–210, 2004/3.

[9] P. C. T. de Boer, "Pressure heat pumping in the optr," *Advances in Cryogenic Engineering*, vol. 41, p. 1373, 1988.

[10] P. Kittel, "Ideal orifice pulse tube refrigerator performance," *Cryogenics*, vol. 32, no. 9, pp. 843–844, 1992.

[11] A. J. Organ, *The Regenerator and the Stirling Engine.* London, UK: JW Arrowsmith Ltd., 1997.

[12] A. J. Organ, pp. 79–85. Thermodynamics and Gas Dynamics of the Stirling Cycle Machine, New York: Cambridge University Press, 1992.

[13] P. J. Storch and R. Radebaugh *Advances in Cryogenic Engineering*, vol. 33, p. 851, 1988.